SUPPLEMENTAL INFORMATION

Supplemental Information includes 7 Figures and 2 Tables and Extended Experimental Procedures.

SUPPLEMENTAL DATA INVENTORY

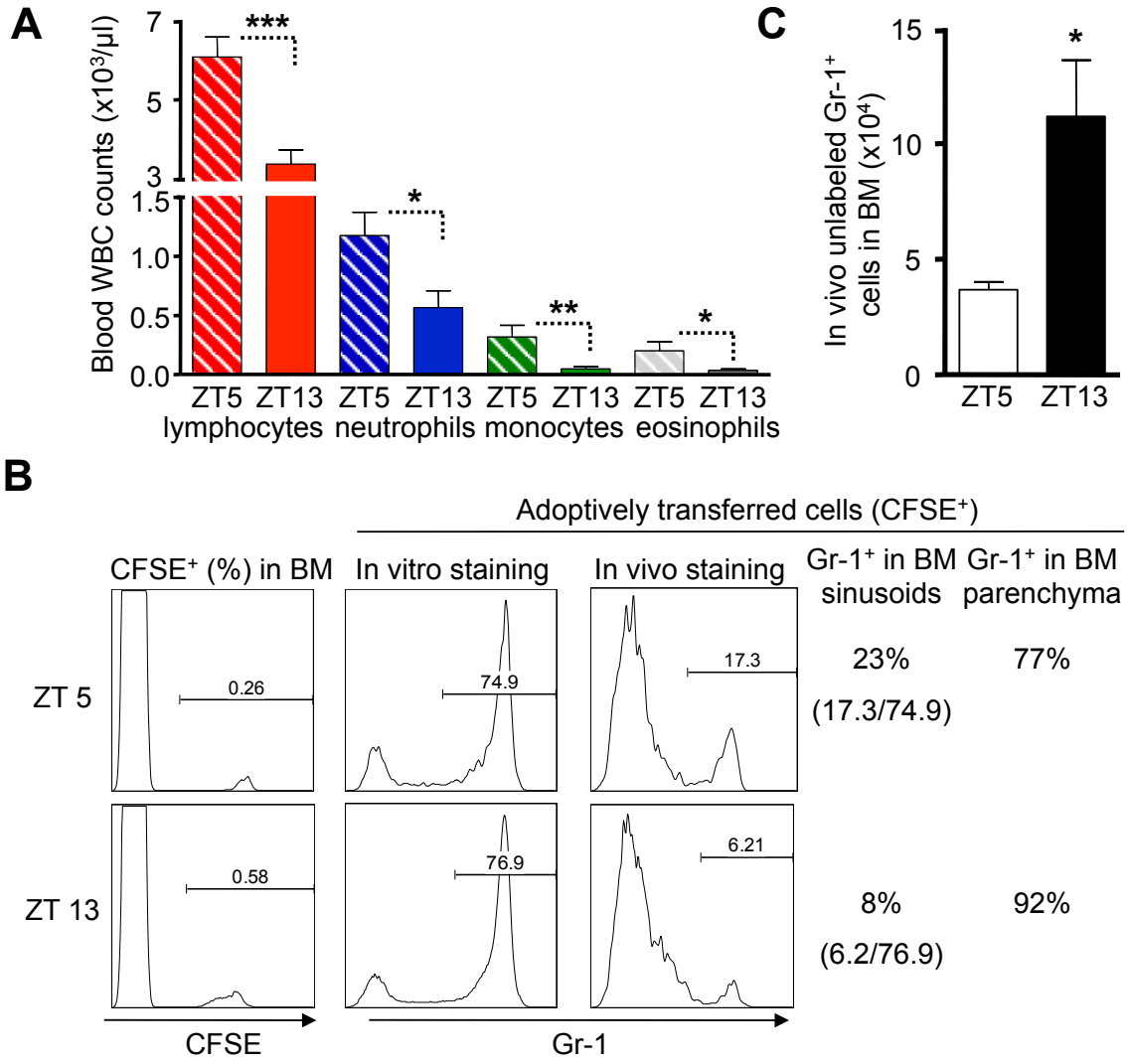

Figure S1

Circadian oscillations in blood leukocyte populations and BM recruitment, Related to Figure 1

(**A**) Circadian oscillations in blood leukocyte populations as analyzed by Wright-Giemsa staining of blood smears at ZT5 and ZT13. n = 10-12. (**B**-**C**) To examine whether adoptively transferred cells were located in the BM parenchyma, mice were injected with fluorescently labeled BM cells, followed by i.v. administration of a fluorochrome-conjugated anti-Gr-1 antibody as described (Pereira et al., 2009). 17.3 % and 6.2 % of

adoptively transferred cells were stained at ZT5 and ZT13 (**B**). These percentages accounted for 23% and 8% of total Gr-1^{+} cells in the transferred fraction whereas 77% and 92% were not stained, respectively. Therefore, more cells residing in the BM parenchyma (unlabeled *in vivo*) were observed at night (**C**), suggesting that most of recruited cells to the BM had migrated into the parenchyma. n = 4-5 mice per group, *P<0.05, **P<0.01, ***P<0.001.

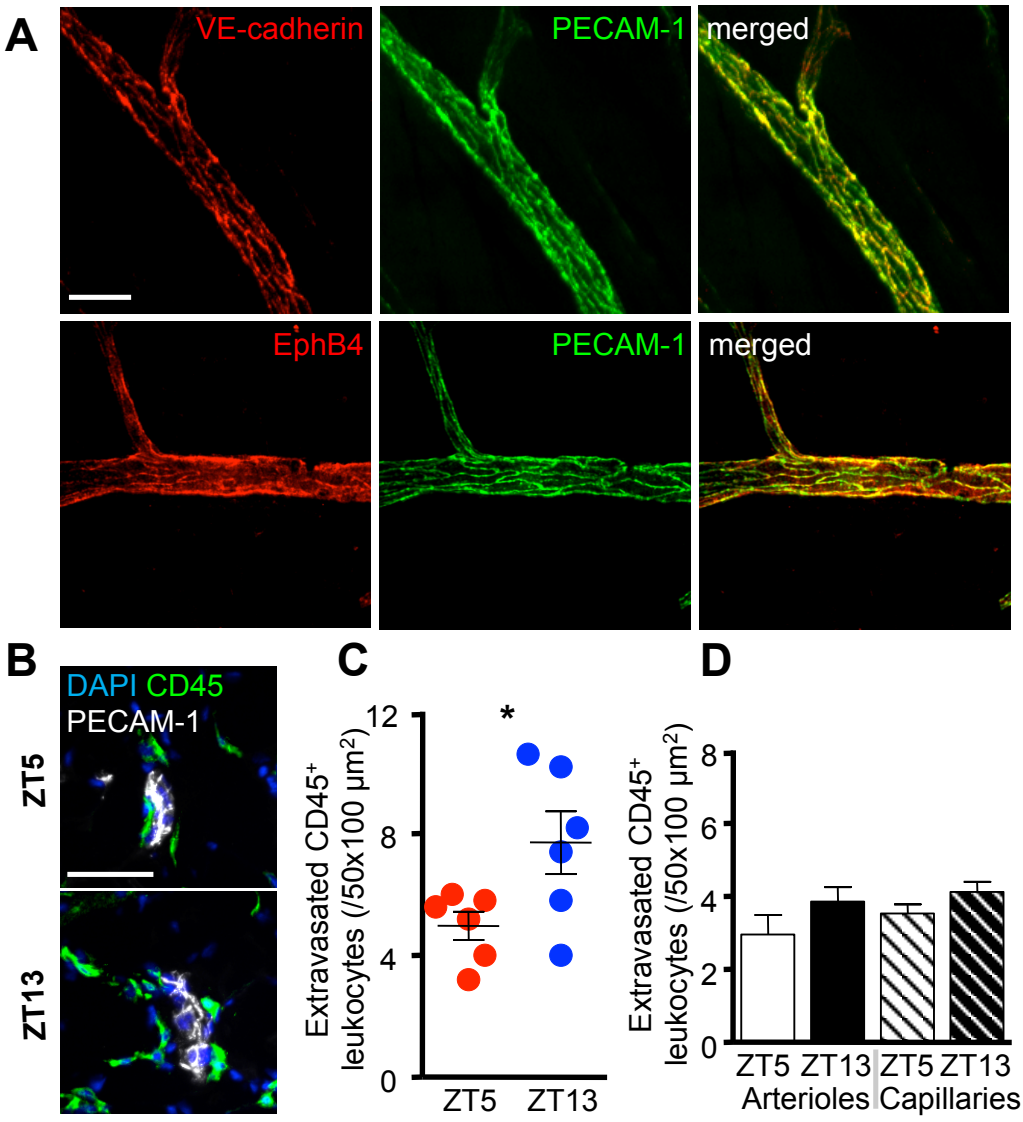

Figure S2

Circadian oscillations in extravascular leukocyte numbers in the cremaster muscle, Related to Figure 2

(**A**) Identification of postcapillary venules by co-expression of the vascular markers PECAM-1 (green), VE-cadherin (red) or EphB4 (red). (**B**-**C**) *Ex vivo* images (**B**) and quantifications (**C**) of extravasated $CD45^+$ leukocytes situated around $PECAM\text{-}1^+$-postcapillary venules quantified by confocal immunofluorescence imaging of frozen cremaster muscle tissue section at ZT5 and ZT13. n = 6. (**D**) Numbers of extravasated

$CD45^+$ leukocytes situated around arterioles and capillaries as analyzed by whole-mount immunofluorescence staining of harvested cremaster muscle tissues. n = 6. *P<0.05. Scale bars: 50 μm,

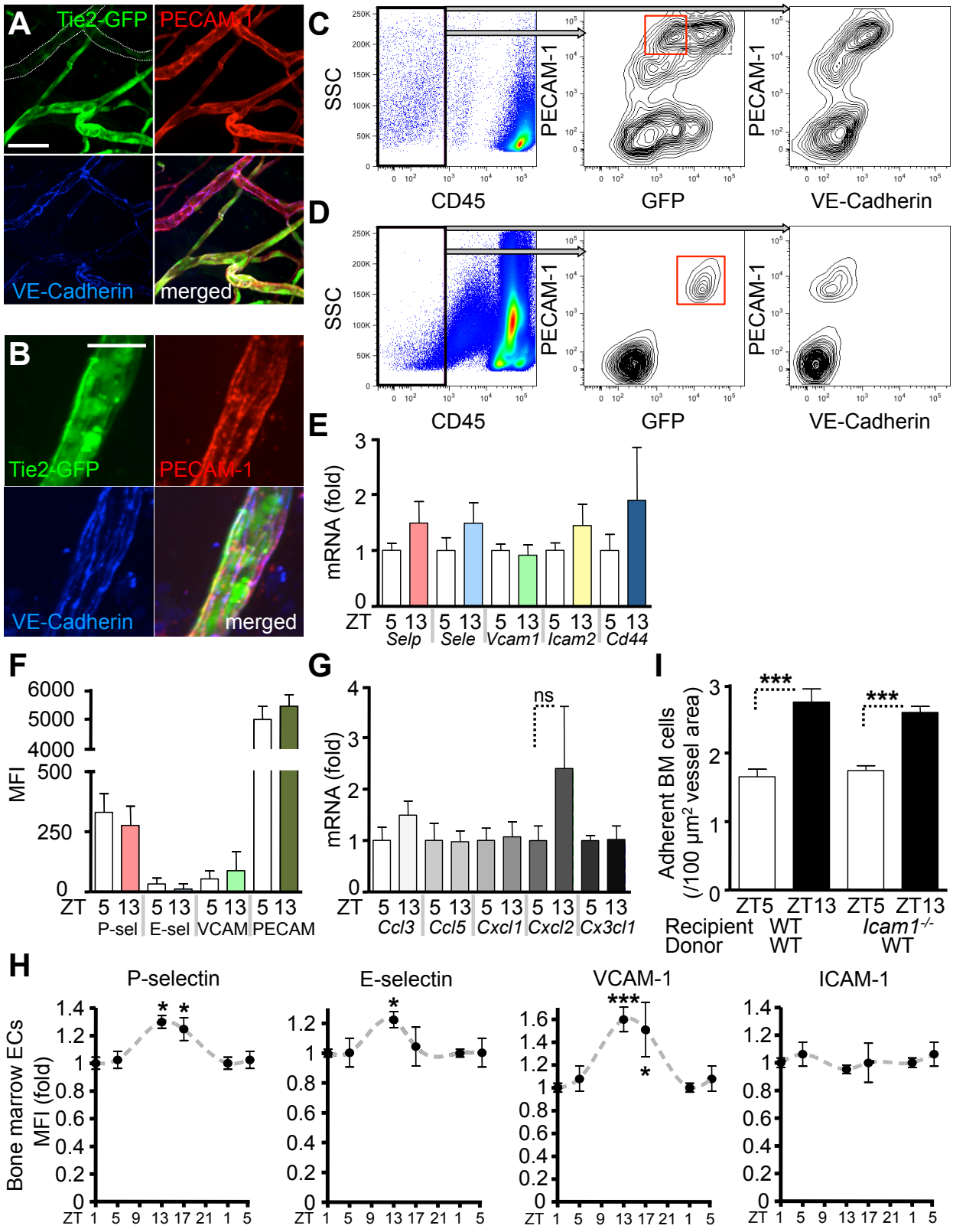
A
Tie2-GFP
PECAM-1
VE-Cadherin
merged
B
Tie2-GFP
PECAM-1
VE-Cadherin
merged
C
SSC
CD45
PECAM-1
GFP
PECAM-1
VE-Cadherin
D
SSC
CD45
PECAM-1
GFP
PECAM-1
VE-Cadherin
E
mRNA (fold)
ZT 5 13 5 13 5 13 5 13 5 13
Selp Sele Vcam1 Icam2 Cd44
F
MFI
ZT 5 13 5 13 5 13 5 13
P-sel E-sel VCAM PECAM
G
mRNA (fold)
ns
ZT 5 13 5 13 5 13 5 13 5 13
Ccl3 Ccl5 Cxcl1 Cxcl2 Cx3cl1
I
Adherent BM cells
(/100 µm² vessel area)
***
***
ZT5 ZT13 ZT5 ZT13
Recipient WT Icam1-/-
Donor WT WT
H
P-selectin
E-selectin
VCAM-1
ICAM-1
Bone marrow ECs
MFI (fold)
ZT 1 5 9 13 17 21 1 5

Figure S3

Circadian oscillations in endothelial cell adhesion molecules and chemokines, Related to Figure 3

(**A-D**) Identification of endothelial cells in cremaster muscle and BM. Whole mount *ex vivo* imaging of the cremaster muscle (**A**) and sternum (**B**) from Tie2-GFP mice co-stained with antibodies directed against PECAM-1 and VE-Cadherin. (**C**-**D**) Gating strategy employed to sort endothelial cells (red gates) in the cremaster muscle (**C**) and BM (**D**). Endothelial cells were identified as being $CD45^-$ VE-$cadherin^+$ $PECAM^+$ as well as $Tie2GFP^{lo}$ (skeletal muscle, **C**) or $Tie2GFP^+$ (BM, **D**) consistent with a previous report in skeletal muscle demonstrating higher Tie2 expression in arteries (grey dotted gate in **C**) than in veins (white dotted lines in **A** and red gate in **C**) (Anghelina et al., 2005). We therefore sorted the $CD45^-$ VE-$cadherin^+$ $PECAM^{HI}$ $Tie2^{lo}$ cremasteric endothelial cells (red gate) to enrich for the venular fraction. (**E**) Q-PCR analysis of cell adhesion molecule expression in sorted cremasteric endothelial cells. n = 12-16. (**F**) Quantification of endothelial cell adhesion molecule expression in skeletal muscle by confocal immunofluorescence imaging of frozen sections. n = 3-6. (**G**) Q-PCR analysis of chemokines in sorted cremasteric endothelial cells. n = 3-6. (**H**) Time course for adhesion molecule expression in BM endothelial cells by flow cytometry. n = 5-15. (**I**) Quantification of fluorescently labeled adherent cells to BM sinusoids of *Icam1*$^{-/-}$ animals after adoptive transfer. n = 54-75 areas from 4 mice per group. *P<0.05, ***P<0.001. Scale bars: (A) 50 μm, (B) 25 μm.

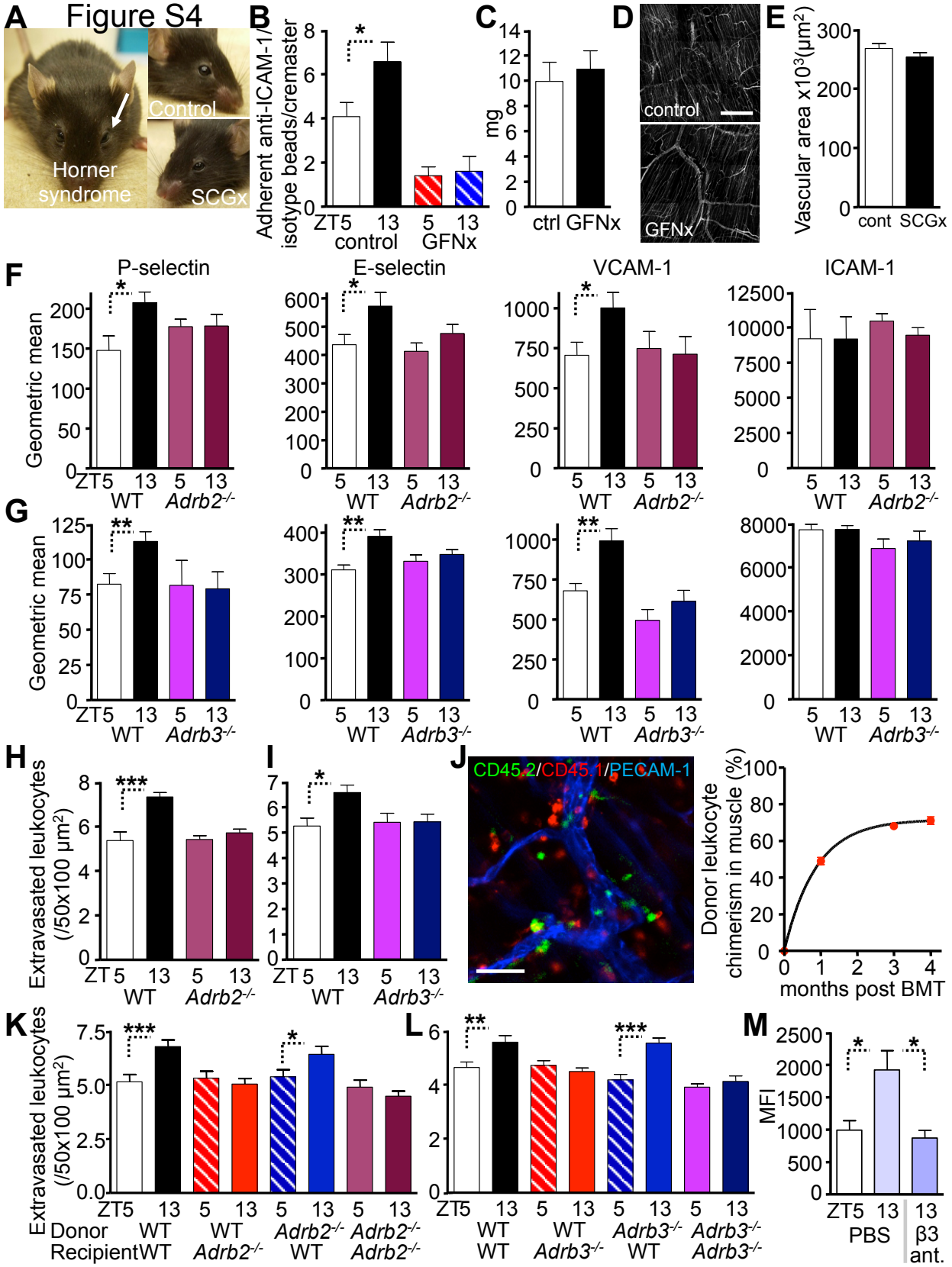
A
Figure S4
Horner syndrome
Control
SCGx
B
Adherent anti-ICAM-1/isotype beads/cremaster
ZT5 13 5 13
control GFNx
C
mg
ctrl GFNx
D
control
GFNx
E
Vascular area x10³(µm²)
cont SCGx
F
P-selectin
E-selectin
VCAM-1
ICAM-1
Geometric mean
WT Adrb2-/-
G
Geometric mean
WT Adrb3-/-
H
Extravasated leukocytes (/50x100 µm²)
WT Adrb2-/-
I
WT Adrb3-/-
J
CD45.2/CD45.1/PECAM-1
Donor leukocyte chimerism in muscle (%)
months post BMT
K
Extravasated leukocytes (/50x100 µm²)
Donor WT WT Adrb2-/- Adrb2-/-
Recipient WT Adrb2-/- WT Adrb2-/-
L
WT WT Adrb3-/- Adrb3-/-
WT Adrb3-/- WT Adrb3-/-
M
MFI
PBS β3 ant.

Figure S4

Effect of loss of functional innervation on circadian oscillations, Related to Figure 4

(**A**) Horner syndrome after unilateral SCGx. (**B**) Quantification of specific (anti-ICAM-1-coated) vs. non-specific (IgG-coated) fluorescent microsphere adhesion in hematopoietic *Icam1*$^{-/-}$/WT BM chimeras in lateral control and GFNx cremaster muscles at ZT5 and ZT13. n = 5-7. (**C**-**D**) Cremaster muscle weight (**C**) and vascular density (**D**) in sham-operated and GFNx muscle tissues. n = 3. (**E**) Quantified vascular areas in sham-operated and SCGx calvarial BM tissues. n = 28-33 areas from 4 mice per group. (**F**-**G**) Flow cytometric analysis of WT control and *Adrβ2*$^{-/-}$ (**F**) or *Adrβ3*$^{-/-}$ (**G**) endothelial BM cells for adhesion molecule expression. n = 6-11. (**H**-**I**) Numbers of extravasated total CD45^{+} leukocytes at ZT5 and ZT13 as analyzed by whole-mount immunofluorescence staining of the cremaster muscle in WT control and *Adrβ2*$^{-/-}$ (**H**) and *Adrβ3*$^{-/-}$(**I**) animals. n = 6-8 mice. (**J**) Representative image of a cremaster muscle tissue harvested from CD45.2 WT recipients four months after BM-transplantation with 10^6 nucleated CD45.1 BM WT cells and whole-mount stained with fluorescence-conjugated antibodies directed against CD45.2 (green), CD45.1 (red) and PECAM-1 (blue). Timecourse of chimerism of extravasated donor hematopoietic cells in cremaster muscle tissues after BM-transplantations as quantified by whole-mount immunofluorescence staining. (**K**-**L**) Numbers of extravasated CD45^{+} leukocytes at ZT5 and ZT13 as analyzed by whole-mount immunofluorescence staining of the cremaster muscle in *Adrβ2*$^{-/-}$/WT (**K**) and *Adrβ3*$^{-/-}$/WT (**L**) BM chimeras. n = 14-32 vessels quantified from 3-6 mice per group. (**M**) Quantification of endothelial cell adhesion

molecule expression in skeletal muscle by confocal immunofluorescence imaging of frozen sections after injection of PBS or the specific β3-antagonist SR59230A. n = 6-11. *P<0.05, **P<0.01, ***P<0.001. Scale bars: (D) 500 μm, (J) 50 μm.

A

Days after BMT	Treatment	Time	WBC x10^6/ml	RBC x10^9/ml	Hgb (g/dl)	HCT %	MCV fL	MCH pg	MCHC g/dL	CHCM g/dL	CH pg	RDW %	HDW g/dL	PLT x10^6/ml	MPV fL
10	none	ZT5	0.28	3.5	4.2	15.4	42	10.6	25.4	31.8	13.1	14.5	3.4	280	36.4
18	none	ZT5	0.05	3.6	5.0	15.7	44	13.9	31.7	30.0	13.1	17.4	2.6	11	11.1
24	none	ZT5	0.80	1.2	1.3	5.2	44	10.7	24.3	27.8	11.7	30.2	5.9	139	19.3
14	PBS	ZT5	0.02	1.9	2.6	7.5	40	13.9	34.3	32.4	13.0	12.5	2.8	6	20.1
14	PBS	ZT5	0.03	4.2	5.9	18.6	44	14.0	31.7	29.4	12.9	11.9	2.1	10	8.4
17	PBS	ZT5	0.03	1.8	2.3	6.8	39	13.3	34.4	33.4	12.8	13.4	3.2	10	18.1

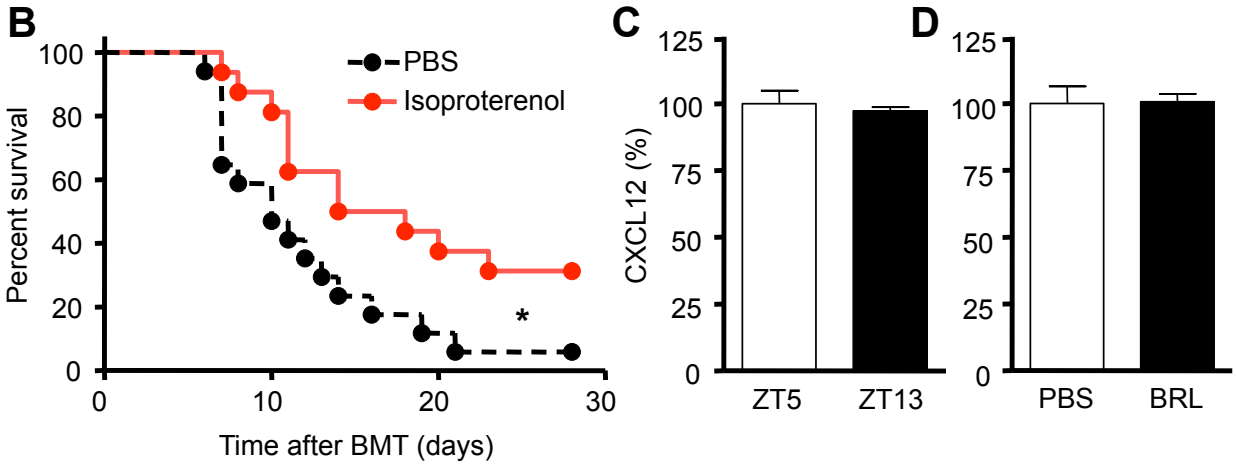

Figure S5

β-agonist-treatment and hematopoietic cell recruitment to the BM, Related to Figure 5

(**A**) Complete blood counts (CBC) of moribund mice after BMT with 2.5x10^4 BM cells at ZT5 (top rows, compared to ZT13) or PBS (bottom rows, compared to BRL37344). WBC: white blood cells; RBC: red blood cells; Hgb: hemoglobin; HCT: hematocrit; MCV: mean cell volume; MCH: mean corpuscular hemoglobin content; MCHC: mean corpuscular hemoglobin concentration; CHCM: cell hemoglobin concentration mean; CH: corpuscular hemoglobin; RDW: red cell distribution width; HDW: hemoglobin distribution width; PLT: platelets; MPV: mean platelet volume. (**B**) Survival curves after transplantation with limiting numbers of BM cells (2.5x10^4) into lethally irradiated

recipients pre-treated with PBS or isoproterenol. n = 16-17. (**C-D**) CXCL12 levels after lethal irradiation and harvest at ZT5 and ZT13 (n = 3-4) (**C**) or after treatment with PBS or BRL37344 (**D**). n = 8-9. *P<0.05.

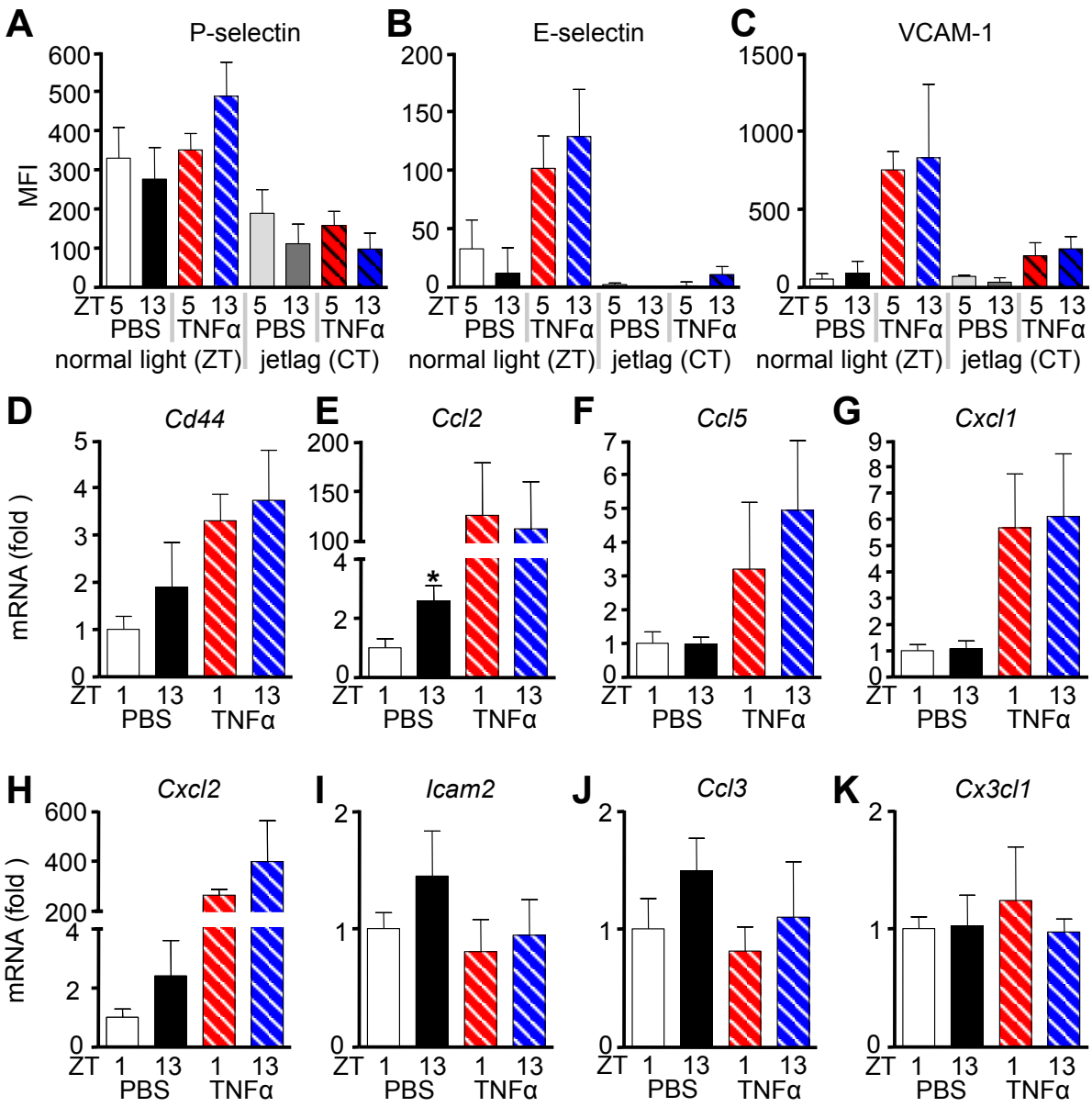

Figure S6

Expression of adhesion molecules and chemokines in cremasteric endothelial cells in steady state and inflammation, Related to Figure 6

(**A**-**C**) Quantification of endothelial cell adhesion molecule expression in skeletal muscle by confocal immunofluorescence imaging of frozen sections at steady state and TNFα-induced inflammation under normal light and jetlag conditions. n = 3-7. (**D**-**K**) Q-PCR

analysis of cell adhesion molecules and chemokines in sorted cremasteric endothelial cells at steady state and TNFα-induced inflammation. n = 3-6. *P<0.05.

Figure S7

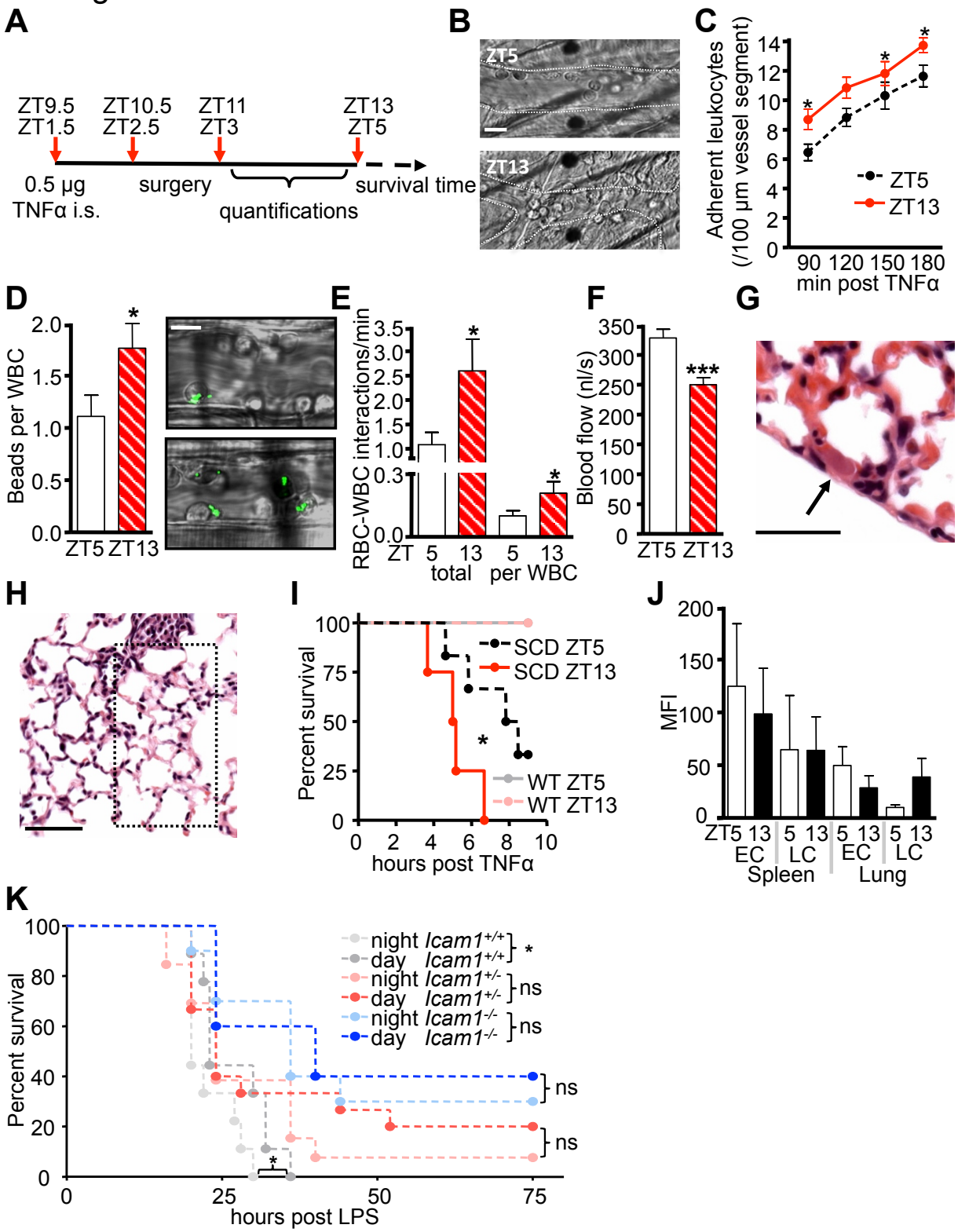
A
ZT9.5
ZT1.5
ZT10.5
ZT2.5
ZT11
ZT3
ZT13
ZT5
0.5 µg
TNFα i.s.
surgery
quantifications
survival time
B
ZT5
ZT13
C
Adherent leukocytes
(/100 µm vessel segment)
ZT5
ZT13
90 120 150 180
min post TNFα
D
Beads per WBC
ZT5 ZT13
E
RBC-WBC interactions/min
ZT 5 13 5 13
total per WBC
F
Blood flow (nl/s)
ZT5 ZT13
G
H
I
Percent survival
SCD ZT5
SCD ZT13
WT ZT5
WT ZT13
hours post TNFα
J
MFI
ZT5 13 5 13 5 13 5 13
EC LC EC LC
Spleen Lung
K
Percent survival
night lcam1+/+
day lcam1+/+
night lcam1+/-
day lcam1+/-
night lcam1-/-
day lcam1-/-
ns
hours post LPS

Figure S7

Circadian rhythms impact inflammatory diseases, Related to Figure 7

(**A**) Experimental design for intravital microscopy experiments in SCD mice. (**B**) Representative *in vivo* images of TNFα-stimulated cremasteric postcapillary venules at ZT5 and ZT13. The vessel-tissue boundary is delineated with a dotted line. (**C-F**) Intravital microscopy experiments quantifying (**C**) leukocyte adhesion, (**D**) Mac-1 activity (as analyzed by fluorescent microsphere capture of adherent leukocytes. n = 43-46 vessels quantified from 8 mice per group), (**E**) WBC-RBC heterotypic interactions (total and per adherent WBC) and (**F**) blood flow. n = 64-96 vessels quantified from 4-6 mice per group. (**G**-**H**) Pathologies observed in SCD mice after stimulation with TNFα. H&E staining of lung sections showing a fibrin microthrombus (**G**) and a focal region of infarction (**H**). (**I**) Survival curves of SCD and WT mice after TNF-α injection. n = 3-6 mice. (**J**) TNF-receptor expression on endothelial cells (EC) and leukocytes (LC) in tissues as quantified by confocal immunofluorescence imaging of frozen sections. n = 3. (**K**) Survival curves of WT, *Icam1*$^{+/-}$ and *Icam1*$^{-/-}$ animals after LPS-induced sepsis (40mg/kg). n = 9-15. *P<0.05, ***P<0.001. Scale bars: (B,D) 10 μm, (G) 25 μm, (H) 50 μm.

Table S1

Tissues	Time	Mice	Venules	Venule diameter (µm)	Centerline velocity (mm/s)	Blood flow rate (nl/s)	Wall shear rate (s^{-1})
Calvarial bone marrow	ZT5	5	21	24.1 ± 1.1	1.3 ± 0.2	383 ± 63	606 ± 81
	ZT13	6	25	24.8 ± 1.4	1.7 ± 0.2	591 ± 109	736 ± 67
Cremaster muscle	ZT5	10	100	27.2 ± 0.9	3.7 ± 0.4	1825 ± 316	1356 ± 128
	ZT13	10	99	29.4 ± 0.6	3.7 ± 0.4	1646 ± 193	1358 ± 129

Investigation of circadian influences on hemodynamic parameters, Related to Figures 1 and 2

Hemodynamic parameters quantified during IVM analysis of the calvarial BM and cremasteric microcirculation at ZT5 and ZT13. All data are represented as mean ± standard error.

Table S2

Treatment	Time	Mice	Venules	Venule diameter (µm)	Centerline velocity (mm/s)	Blood flow rate (nl/s)	Wall shear rate (s^{-1})
sham	ZT5	3	28	28.1 ± 1.3	3.3 ± 0.4	1317 ± 198	1311 ± 170
	ZT13	4	40	30.1 ± 1.0	3.6 ± 0.5	1795 ± 257	1277 ± 177
GFNx	ZT5	3	30	29.7 ± 0.8	3.7 ± 0.5	1708 ± 241	1343 ± 153
	ZT13	4	39	29.0 ± 0.9	3.7 ± 0.3	1675 ± 197	1391 ± 127

Investigation of circadian influences on hemodynamic parameters after GFNx, Related to Figure 4

Hemodynamic parameters quantified during IVM analysis of the cremasteric microcirculation at ZT5 and ZT13 in contralateral and GFNx cremaster muscle tissues. All data are represented as mean ± standard error.

EXTENDED EXPERIMENTAL PROCEDURES

Animals

Bmal1$^{-/-}$ (Bunger et al., 2000), *Adrb2*^{tm1Bkk} (Chruscinski et al., 1999), *SeleSelp*$^{-/-}$ (Frenette et al., 1996), FVB/N-*Adrb3*^{tm1Lowl}/J (Susulic et al., 1995), *Icam1*^{tm1Jcgr}/J (Xu et al., 1994), *Vav1-cre*^{A2Kio}/J, STOCK Tg(TIE2GFP)287Sato/J (Motoike et al., 2000) mice (all from Jackson Laboratories), and *ROSA26Sor*$^{tm2(ACTB-Luc)Tyj}$ and the inbred FVB/NJ and C57BL/6-CD45.1/2 congenic strains (National Cancer Institute) were used in this study. Berkeley SCD mice [Tg(Hu-miniLCRα1$^{G}\gamma^{A}\gamma\delta\beta^{S}$) *Hba*$^{-/-}$ *Hbb*$^{-/-}$], have been previously described (Paszty et al., 1997). Bone marrow nucleated cells from Berkeley SCD mice were transplanted into lethally irradiated C57BL/6 animals to generate age- and gender-matched genetically identical cohorts of SCD mice. Fully chimeric male SCD mice (expressing >97% human globin, including Hb^{S}) were subjected to BIM 3-5 months after bone marrow transplantation as previously described (Turhan et al., 2002).

Antibodies

PE/PE-Cy7-anti-CD45 (30-F11), PE/APC-anti-F4/80 (CI:A3-1), APC-anti-PECAM-1 (Mec13.3), FITC/PE/PE-Cy7-anti-CD45.1 (A20), FITC/PE-anti-CD45.2 (104), PE-anti-CD106 (429), APC/FITC-anti-Gr-1 (RB6-8C5) (all Biolegend); PE-anti-mouse/human CD62P (KO2.3), PE/Cy7-anti-CD117 (289), FITC-anti-Ly6A/E (D7), Alexa647-anti-VE-Cadherin (BV13), biotin-anti-ICAM-1 (YN1/1.7.4), biotin-isotype control (eB149-10H5) (both eBioscience); PE-anti-CD62E (10E9.6), PE-anti-CD11b (M1/70), PE-rat control isotype, biotin-anti-Lineage (TER-119, RB6-8C5, RA3-6B2, M1/70, 145-2C11) (all BD Pharmingen). PE-anti-LYVE-1 (ALY7) (MBL); pAb anti-TH (AB152) (Millipore) in

combination with the Tyramide Signal Amplification kit (Perkin Elmer); pAb anti-Ki67 (Novus Biologicals) in combination with secondary Alexa488-anti-rabbit ab (Invitrogen).

In vivo injection of antibodies

Anti-VCAM-1 antibody (clone M/K 2.7) and control rat IgG were obtained from Bio-XCell. Animals were injected intravenously with 1 mg kg^{-1} of each antibody or equivalent amounts of rat IgG. For homing experiments, recipient mice were injected intravenously with 1 mg kg^{-1} of anti-VCAM-1 antibody (clone M/K 2.7) 12 h and 2 h before transfer of donor cells.

Blood leukocyte counts

Blood was harvested from anesthetized mice through the retro-orbital plexus, collected in EDTA and analyzed on a Beckman coulter counter AcT diff (Beckman) or ADVIA 120 hematology system (SIEMENS).

Histopathology

Lung and liver were excised and fixed in 10% neutral buffered formalin for 36-72 hours and routinely processed for paraffin embedding. Samples for histopathology diagnostics were sectioned to a thickness of 5µm and stained routinely using hematoxylin and eosin (H&E) stains and evaluated by a board certified veterinary pathologist.

Intravital microscopy

Brightfield intravital microscopy (BIM)

Male mice were anesthetized by intraperitoneal (i.p.) injection of a mixture of 2% chloralose (Sigma) and 10% urethane (Sigma) in PBS. A polyethylene tube was inserted into the trachea to facilitate spontaneous respiration. The cremaster muscle was gently exteriorized, pinned out over the optical window of a microscopic stage and then continuously superfused throughout the experiment with warmed (37°C) bicarbonate-buffered (pH 7.4) saline aerated with a 95/5% N_2/CO_2 mixture. To observe leukocyte/endothelial cell interactions, post-capillary venules, ranging from 20-40 µm in diameter, were identified and leukocyte rolling, firm adhesion and transmigration were quantified on a custom-designed upright microscope (MM-40, Nikon), using a 60X water immersion objective (Nikon). Rolling flux was quantified as the number of rolling cells crossing an imaginary line per minute. Firmly adherent leukocytes were considered as those remaining stationary for at least 30 s within a given 100 µm vessel segment. Extravasated leukocytes were quantified as those in a perivascular area along 100 µm vessel segments and within 50 µm in the tissue. Multiple vessels (6-10) were studied for each animal. Images were recorded using a charge-coupled device video camera (Hamamatsu) and video recorder (Sony SVHS, SVO-9500). Offline analysis was performed using Pinnacle software.

Brightfield microscopy of SCD mice

For investigations of SCD mice, animals were injected i.s. with 0.5 µg TNF-α (R&D Systems) and 90 min later the leukocyte response in the cremaster muscle was

quantified as described above with each venule recorded continuously for at least 2 min over a period of 120 min. Survival time was recorded (max 9h) defined as the time from TNF-α injection until death of the mouse.

Hemodynamic measurements and image analysis for brightfield intravital microscopy

Venular diameter was measured with a video caliper. Centerline red cell velocity (V_{RBC}) was measured for each venule in real time using an optical Doppler velocimeter (Texas A&M). Wall shear rate (γ) was calculated based on Poiseuille's law for a Newtonian fluid, $\gamma = 2.12\ (8V_{mean}) / D_v$, where D_v is the venular diameter, V_{mean} is estimated as V_{RBC} / 1.6, and 2.12 is a median empirical correction factor obtained from actual velocity profiles measured in micro- vessels *in vivo*. Blood flow rate (Q) was calculated as $Q = V_{mean}\ \pi d^2/4$, where d is venule diameter, and is expressed as nl/s. An interaction between RBCs and adherent WBCs was defined as the association between an RBC and an adherent WBC for more than 2 video frames (> 0.07 second). This time interval corresponds to a readily discernable adhesion event when the videotape is played in real time. We performed all analyses by playback assessment of videotapes as previously described (Chang et al., 2008; Turhan et al., 2002).

Multichannel fluorescence intravital microscopy (MFIM)

Cremaster muscle

Mice were injected i.v. with low doses of fluorescently conjugated antibodies (FITC-anti-Gr-1, APC-anti-F4/80 and PE-anti-CD45; 0.1-0.5 μg/mouse) and the numbers of

adherent leukocytes were quantified on an Olympus BX61WI microscope equipped for epifluorescence imaging as previously described (Scheiermann et al., 2007).

Quantification of adherent microspheres by MFIM

Yellow-green or red fluorescent NeutrAvidin-coated microspheres (1.1 µm-diameter; Invitrogen) were sonicated and incubated overnight with biotinylated anti-ICAM-1 or isotype control antibody, thoroughly washed and resuspended in PBS for a final concentration of 0.2% solids = 0.002 g/ml according to the manufacturer's protocol. 10^7 beads each were co-injected into anesthetized mice prepared for MFIM. Numbers of adherent beads (> 30s interaction time) were quantified per cremaster muscle and the ratio of specific vs. unspecific beads was plotted. The assay quantifying Mac-1 integrin activity using BSA-coated fluorescent microspheres was performed as previously detailed (Hidalgo et al., 2009).

Calvarial bone marrow

We performed MFIM of the calvarial BM as previously described (Mazo et al., 1998). In adoptive transfer experiments, all images were acquired with an Olympus BX61WI microscope and analyzed with Slide Book software (Intelligent Imaging Innovations). Endogenous leukocytes and BM sinusoids were visualized by administration of 10 µg of rhodamine 6G (R6G; Sigma). Leukocyte rolling was quantified with a custom-designed Nikon MM-40 microscope (Nikon, Tokyo, Japan). Images were analyzed using a charge-coupled device video camera (Hamamatsu, Bridgewater, NJ) and a Sony SVHS SVO-9500 video recorder (Sony, Tokyo, Japan) as described previously (Turhan et al.,

2002). The rolling flux fraction is defined as the fraction of rolling cells versus total blood leukocyte counts.

Bioluminescence Imaging

Mice were i.v. injected at different ZTs with 10^7 BM cells harvested at the same ZT from Vav1-*Cre; Rosa26*-lsl-*Luc* mice expressing luciferase selectively in hematopoietic cells. 1h after adoptive transfer recipients were i.p. injected with 300 mg/kg luciferin. 15 minutes later, livers were harvested and imaged on an IVIS-Imaging system (Caliper Life Sciences). Analyses were performed using Living Image 4.0 Software. Data was plotted as Average Radiance, which is the sum of the radiance from each pixel inside the ROI/number of pixels (photons/sec/cm2/sr).

Surgical denervation techniques

Genitofemoral nerve surgery

Mice were anesthetized with avertin (375 mg/kg), a midline incision was made along the abdomen and the intestine was gently pulled out from the abdominal cavity as previously described in rats (Lucio et al., 2001; Sachs and Liu, 1992; Tiryaki et al., 2000). The GFN was identified running alongside the aorta on top of the psoas major muscle and was cut between the renal and iliac artery before branching into its femoral and genital components. A large lesion was made to prevent nerve regeneration. The intestine was returned to its normal position, the abdominal incision was closed with a monofilament suture and mice were left to recover for four weeks to re-establish leukocyte homeostasis.

Surgical denervation of cervical sympathetic nerves

Under anesthesia using avertin, a ventral neck incision was made to localize the carotid bifurcation. The ganglion was identified underneath the bifurcation. The SCG and sympathetic tract were transected unilaterally. Mice were left to recover for 4 weeks to re-establish systemic homeostasis. After the surgical procedures mice were left to recover for four weeks when leukocyte numbers and rhythms in blood were similar to unstimulated wild-type animals indicating the absence of acute inflammation and the re-establishment of leukocyte homeostasis.

Whole-mount immunofluorescence

Tissues were dissected away from mice, fixed in methanol, blocked/permeabilized in PBS supplemented with 20 % normal goat serum (NGS) and 0.5 % Triton X-100, and incubated with fluorescence-conjugated antibodies. Tissues were imaged on an Olympus BX61WI microscope equipped for epifluorescence imaging or on an Axio Examiner.D1 microscope (Zeiss) equipped with a Yokogawa CSU-X1 confocal scan head with four stack laser system (405nm, 488nm, 561nm, and 642nm wave lengths). Images were obtained as 3D stacks scanning through the whole thickness of the tissue using Slidebook software (Intelligent Imaging Innovations). Extravasated leukocytes were quantified within 50 µm to postcapillary venules along the whole length of imaged vessels. Calvarial or sternal bones were fixed in methanol or 4% paraformaldehyde, blocked / permeabilized in PBS containing 20% normal goat serum and 0.5% Triton X-100 and stained with primary antibodies. For TH staining, we incubated tissues with biotinylated anti-rabbit antibody and amplified signals with the ABC-Cy3 tyramide

fluorescence enhance kit (Perkin Elmer) as indicated in the manufacturer's instructions or using a fluorochrome-conjugated anti-rabbit antibody (invitrogen).

Immunofluorescence on frozen sections

Tissues from untreated, TNFα (0.5μg)-, PBS- or the specific β3-antagonist SR59230A (2mg/kg)-treated animals were embedded in OCT, snap frozen in liquid nitrogen and sectioned on a cryostat (Leica). Sections were fixed, incubated with fluorescently coupled antibodies and imaged as detailed above. For investigations of expression levels, all quantifications were performed using mask analysis (Slidebook, Intelligent Imaging Innovations) based on PECAM-1 expression and quantifying expression of other fluorescent channels within the mask containing $PECAM^+$-pixels delineating vascular structures. All images were acquired by confocal microscopy as detailed above.

Homing assay of HSPCs

BM cells were harvested from recipients 3h after donor BM cells ($5x10^6$) were injected. For circadian experiments, a group of mice was housed in a chamber with a shifted light-dark cycle to compare ZT1 and ZT13 or ZT5 and ZT17 at the same circadian time. Homing of donor BM and LSK cells were assessed with congenic CD45.1/2 mice by flow cytometry. For progenitor homing assessed by CFU-C cultured in methylcellulose (MethoCult M3534; StemCell Technologies), recipient mice were given 13 Gy irradiation. The number of homed CFU-Cs per femur was corrected to represent the whole BM (multiplied by 16.9 because one femur represents approximately 5.9% of the

total murine BM) as previously described (Katayama et al., 2003). Mice not injected with donor cells were used for background controls.

Competitive reconstitution assay for LT-HSC homing

5 x 10^6 CD45.1 BM cells were transplanted into lethally irradiated CD45.2 recipients pre-treated with BRL37344 (5mg/kg) or PBS. One day later, BM cells were harvested from a femur and transplanted into secondary recipients with 2x10^5 competitive CD45.2 BM cells. CD45.1 cells in peripheral blood in secondary recipients were assessed for 16 weeks after transplant.

Q-PCR

For Q-PCR equal numbers of endothelial cells were directly sorted into Dynabead lysis/binding buffer (Invitrogen) and frozen at -80ºC. Frozen samples were incubated with polyT magnetic Dynabeads (Invitrogen) and mRNA was harvested according to the manufacturer's protocol. cDNA was prepared by conventional reverse transcription using the Sprint PowerScript reverse transcriptase (Clontech). Q-PCR was performed with SYBR Green on an ABI PRISM 7900HT Sequence Detection System (Applied Biosystems) in accordance to the manufacturer's instructions. Primers were designed with the Primer Express software (Applied Biosystems) and when possible were selected to span introns to prevent the amplification of contaminating genomic DNA. A primer concentration of 300 nM was found to be optimal in all cases. The sequences of the oligonucleotides used are included below. The PCR protocol consisted of one cycle at 95°C (10min) followed by 40 cycles of 95°C (15s) and 60°C (1min). A dissociation

curve analysis was included after each experiment to confirm the presence of a single product and the absence of primer dimers. Expression of *β-actin* and *glyceraldehyde-3-phosphate dehydrogenase* (*Gapdh*) was used as a standard. The average threshold cycle number (C_t) for each tested mRNA was used to quantify the relative expression of each gene: $2^{-[Ct(\text{gene}) - Ct(\text{standard})]}$.

Q-PCR primer sequences

Primers	Sequence	Annealing(°C)
*Selp*_F	GGTATCCGAAAGATCAACAATAAGTG	60
*Selp*_R	GTTACTCTTGATGTAGATCTCCACACA	
*Sele*_F	CCCTGCCCACGGTATCAG	60
*Sele*_R	CCCTTCCACACAGTCAAACGT	
*Vcam1*_F	GACCTGTTCCAGCGAGGGTCTA	60
*Vcam1*_R	CTTCCATCCTCATAGCAATTAAGGTG	
*Icam1*_F	GGACCACGGAGCCAATTTC	60
*Icam1*_R	CTCGGAGACATTAGAGAACAATGC	
*Icam2*_F	ACGTGTTCGGGAAAGCAGCA	60
*Icam2*_R	CAGGGGACACCGTGCACTCA	
*Cd44*_F	ATCAGCAGATCGATTTGAATGTAA	60
*Cd44*_R	CATTTCCTTCTATGAACCCATACC	
*Ccl2*_F	GAGTAGGCTGGAGAGCTACAAGAG	60
*Ccl2*_R	AGGTAGTGGATGCATTAGCTTCAG	
*Ccl3*_F	CCAAGTCTTCTCAGCGCCAT	60
*Ccl3*_R	TCCGGCTGTAGGAGAAGCAG	
*Ccl5*_F	TGGAGATGAGCTAGGATAGAGG	60
*Ccl5*_R	AGTAGGGGATTACTGGAGTGG	
*Cxcl1*_F	GCTGGGATTCACCTCAAGAA	60
*Cxcl1*_R	TCTCCGTTACTTGGGGACAC	
*Cxcl2*_F	CGCTGTCAATGCCTGAAG	60
*Cxcl2*_R	GGCGTCACACTCAAGCTCT	
*Cx3cl1*_F	ACGAAATGCGAAATCATGTGC	60
*Cx3cl1*_R	CTGTGTCGTCTCCAGGACAA	
*β-actin*_F	GCTTCTTTGCAGCTCCTTCGT	60
*β-actin*_R	ATCGTCATCCATGGCGAACT	
*GAPDH*_F	TGTGTCCGTCGTGGATCTGA	60
*GAPDH*_R	CCTGCTTCACCACCTTCTTGA	

CXCL12 ELISA

ELISA plates (96-well) were coated overnight at 4°C with 50 µl of 2 µg/ml anti-CXCL12 coating antibody (MAB350; R&D Systems). Next, the wells were washed three times with wash buffer (0.05% Tween 20 in PBS) and incubated for 1 h at room temperature with 200 µl of blocking buffer (1% BSA, 5% D-Sucrose, and 0.05% NaN3 in PBS; all from Thermo Fisher Scientific). After 3 washes, 100 µl of samples diluted 1:2 in PBS were added and incubated for 2 h at room temperature. After 3 washes, 100 µl of 0.25 µg/ml polyclonal biotinylated anti-human/mouse SDF-1 (BAF310; R&D Systems) was added and incubated for 2 h at room temperature. After 3 washes, 100 µl of 0.1 µg/ml Neutravidin-HRP (Thermo Fisher Scientific) was added and incubated for 30 min. After 3 additional washes, the reaction was developed by incubation for 20-30 min with 50 µl of TMB substrate solution (Sigma-Aldrich) and stopped by adding 50 µl of 1M HCl solution (Thermo Fisher Scientific). Optical density was determined with a microplate reader set at 450 nm. Optical density of PBS control wells was subtracted from optical density of samples. Recombinant mouse SDF-1α (PeproTech) was used to generate a linear standard curve.

Supplemental References

Anghelina, M., Moldovan, L., and Moldovan, N.I. (2005). Preferential activity of Tie2 promoter in arteriolar endothelium. J Cell Mol Med *9*, 113-121.

Bunger, M.K., Wilsbacher, L.D., Moran, S.M., Clendenin, C., Radcliffe, L.A., Hogenesch, J.B., Simon, M.C., Takahashi, J.S., and Bradfield, C.A. (2000). Mop3 is an

essential component of the master circadian pacemaker in mammals. Cell *103*, 1009-1017.

Chruscinski, A.J., Rohrer, D.K., Schauble, E., Desai, K.H., Bernstein, D., and Kobilka, B.K. (1999). Targeted disruption of the beta2 adrenergic receptor gene. J Biol Chem *274*, 16694-16700.

Paszty, C., Brion, C.M., Manci, E., Witkowska, H.E., Stevens, M.E., Mohandas, N., and Rubin, E.M. (1997). Transgenic knockout mice with exclusively human sickle hemoglobin and sickle cell disease. Science *278*, 876-878.

Pereira, J.P., An, J., Xu, Y., Huang, Y., and Cyster, J.G. (2009). Cannabinoid receptor 2 mediates the retention of immature B cells in bone marrow sinusoids. Nature immunology *10*, 403-411.

Sachs, B.D., and Liu, Y.C. (1992). Copulatory behavior and reflexive penile erection in rats after section of the pudendal and genitofemoral nerves. Physiol Behav *51*, 673-680.

Susulic, V.S., Frederich, R.C., Lawitts, J., Tozzo, E., Kahn, B.B., Harper, M.E., Himms-Hagen, J., Flier, J.S., and Lowell, B.B. (1995). Targeted disruption of the beta 3-adrenergic receptor gene. J Biol Chem *270*, 29483-29492.

Tiryaki, T., Abbasoglu, L., and Sakiz, D. (2000). Divison of the genitofemoral nerve in normal scrotal testicular rats. Pediatr Surg Int *16*, 573-575.